Biosensors and Bioelectronics 31 (2012) 349–356

Contents lists available at SciVerse ScienceDirect

Biosensors and Bioelectronics

journal homepage: www.elsevier.com/locate/bios

Development of a multilayered polymeric DNA biosensor using radio frequency technology with gold and magnetic nanoparticles

Cheng-Hao Yang[a], Long-Sheng Kuo[a], Ping-Hei Chen[a,*], Chii-Rong Yang[b], Zuo-Min Tsai[c]

[a] Department of Mechanical Engineering, National Taiwan University, Taipei 106, Taiwan
[b] Department of Mechatronic Technology, National Taiwan Normal University, Taipei 106, Taiwan
[c] Graduate Institute of Communication Engineering and Department of Electrical Engineering, National Taiwan University, Taipei 106, Taiwan

ARTICLE INFO

Article history:
Received 7 July 2011
Received in revised form 11 October 2011
Accepted 24 October 2011
Available online 31 October 2011

Keywords:
Polymeric biosensor
Radio-frequency
DNA detection
Multilayered biosensor

ABSTRACT

This study utilized the radio frequency (RF) technology to develop a multilayered polymeric DNA sensor with the help of gold and magnetic nanoparticles. The flexible polymeric materials, poly (p-xylylene) (Parylene) and polyethylene naphtholate (PEN), were used as substrates to replace the conventional rigid substrates such as glass and silicon wafers. The multilayered polymeric RF biosensor, including the two polymer layers and two copper transmission structure layers, was developed to reduce the total sensor size and further enhance the sensitivity of the biochip in the RF DNA detection. Thioglycolic acid (TGA) was used on the surface of the proposed biochip to form a thiolate-modified sensing surface for DNA hybridization. Gold nanoparticles (AuNPs) and magnetic nanoparticles (MNPs) were used to immobilize on the surface of the biosensor to enhance overall detection sensitivity. In addition to gold nanoparticles, the magnetic nanoparticles has been demonstrated the applicability for RF DNA detection. The performance of the proposed biosensor was evaluated by the shift of the center frequency of the RF biosensor because the electromagnetic characteristic of the biosensors can be altered by the immobilized multilayer nanoparticles on the biosensor. The experimental results show that the detection limit of the DNA concentration can reach as low as 10 pM, and the largest shift of the center frequency with triple-layer AuNPs and MNPs can approach 0.9 and 0.7 GHz, respectively. Such the achievement implies that the developed biosensor can offer an alternative inexpensive, disposable, and highly sensitive option for application in biomedicine diagnostic systems because the price and size of each biochip can be effectively reduced by using fully polymeric materials and multilayer-detecting structures.

1. Introduction

The molecular diagnostics have been extensively applied in numerous fields, such as analytical chemistry, biomedical diagnostics, and anti-bioterrorism diagnostic applications, including DNA detection, system-on-a-chip, and cell and protein molecule diagnostics. Nam et al. (2004) developed several DNA detection assays by using radioactive labels, molecular fluorophores, chemiluminescence schemes, electrochemical tags, and nanostructure-based labels. The technique of the nanostructure-based biosensors is currently being spread out from the laboratory to the clinic, and has the potential to be included in regular medical testing, depending on several scientific factors such as sensitivity, selectivity, and versatility (Giljohann and Mirkin, 2009). The nanoparticles (NPs) exhibit excellent performance that result from cooperative binding properties, unique optical properties, catalytic properties, and the existence of robust and versatile surface-functionalization methods for DNA detection and protein biomedical detection systems (Alivisatos, 2004; Stoeva et al., 2006; Tokonami et al., 2008). The oligonucleotide-functionalized gold nanoparticles (AuNPs) and magnetic nanoparticles (MNPs) have demonstrated advantages on sensitivity and selectivity over conventional probes in a variety of biodetection schemes (Giljohann et al., 2010; Pal and Alocilja, 2010; Kim et al., 2011).

In addition, the bioactive polymeric materials and novel detection methods were extensively developed to achieve rapid, reliable, and high-sensitivity biodetection because of the requirements of lower cost, mass, power consumption, and fewer biological molecules in a biomedical system (Blacklock et al., 2009; Anderson et al., 2005). The polymers form the basis of new platforms for the trace detection of analytes in a variety of biomedical monitoring, such as in DNA and protein detection. The biocompatibility is a vital characteristic of biomedical polymeric materials, the surface of which is required to interact with a biological system (Tirrel

* Corresponding author at: Department of Mechanical Engineering, National Taiwan University, No. 1, Roosevelt Rd Sec. 4, Taipei 10617, Taiwan.
Tel.: +886 2 33662689; fax: +886 2 23670781/23631755.
E-mail address: phchen@ntu.edu.tw (P.-H. Chen).

0956-5663/$ – see front matter © 2011 Elsevier B.V. All rights reserved.
doi:10.1016/j.bios.2011.10.044

et al., 2002). When polymeric biomaterials are in contact with a biological environment, the surface chemistry and topography of the materials are significant parameters that may influence protein adsorption, DNA immobilization, and cell interaction (Ratner and Bryant, 2004). The Parylene-C biomaterial is commonly used as polymeric biomaterials for DNA, cell, and protein detection because Paryelene-C satisfies the requirements such as low background fluorescence, biocompatibility, high chemical resistivity, transparency, and effective adhesion to molecules (Zheng et al., 2007; Chang et al., 2007a).

A biosensor usually consists of a receptor and a transducer for molecular recognition and for converting the information into an electrical signal (Sheehan and Whitman, 2005). The transducer may use optical (Mallard et al., 2005), electrochemical (Wang et al., 2009a), piezoelectric (Wang et al., 2009b), magnetic (Schotter et al., 2004), and electrical detection (Tsai et al., 2006) methods. The functional nanoparticles, that is, metal or semiconductor nanoparticles are widely used to amplify the detected electrical signals caused by the excellent electrical properties of the functional nanoparticles for biomedical detection (Park et al., 2002; Chang et al., 2007b). The optical-, electrochemical-, and piezoelectric-sensing techniques are widely used as DNA detection methods, and the excellent detection limit or sensitivity of these sensing techniques with a signal enhancement of the functional nanoparticles are approximately 5 pM–100 fM (optical method), 10 pM to 500 fM (electrochemical or electrical method), and 1 pM to 100 fM (piezoelectric method) (Agasti et al., 2010; Drummond et al., 2003).

The radio frequency electrical detection method for biomedical systems has been widely developed because the RF electrical detection methods and designs that are integrated with a transmission line, inductive component, and a capacitive component are effective and powerful as a label-free detection system (Kim et al., 2006; Chien et al., 2007; Perng et al., 2007). However, these RF electrical detection methods have not been applied with polymeric biomaterials for biomedical detection, such as DNA detection.

This study is then to develop a sensitive polymeric biosensor by integrating a radio frequency electrical approach with AuNPs and MNPs to enhance the detecting signals from a markedly low concentration of target DNA. Three main objectives are considered for the development of the biosensor in this study. The first objective is to use the frequency response of the developed RF biosensor for detecting the conjugated DNA–AuNPs and DNA–MNPs in biomedical diagnostics since the radio frequency response of the biosensor with conjugated biomolecules is more intensive than the dc or low-frequency response (Kim et al., 2006). The specific immobilization and hybridization among the probe DNA, target DNA, and capture DNA result in the formation of self-assembled AuNPs/MNPs on the sensing surface of the coplanar waveguide (CPW). These nanoparticles will cause the shifting of center resonant frequency.

The second objective is to amplify the signals by using multilayered AuNPs or MNPs. The establishment of multilayered AuNPs or MNPs changes the center frequency of the developed filter. This change indicates the existence of target DNA in the sample solution during the hybridization and immobilization procedures.

The third objective is to develop the multilayered polymeric biosensor, including the two polymer layers, Parylene-C and PEN, and two copper transmission structure layers. The polymeric substrates in general imply the advantages of low cost. The proposed RF biosensor is then designed and fabricated by the two copper transmission structure layers and two polymer materials layers. The size of the microwave device can be reduced by using a multilayer device structure such as that of the proposed biosensor (Huang et al., 2009). The two copper transmission structures with 3D configuration, one upper and one lower layers, can increase the sensing area that is added from the single capacitor structure to the double capacitor structures, and the sensitivity may be further enhanced. Therefore, the multilayer RF biosensor is expected to achieve higher sensitivity and a small chip-size for DNA diagnostics. The advantages of lower cost, effective miniaturization, and higher sensitivity can make the developed biosensor competitive with other biosensors.

2. Experiments

2.1. Polymeric biochip fabrication processes

The multilayered polymeric RF biosensor was fabricated by using micromachining technologies, including polymer and metal deposition, isotropic wet etching, plasma surface treatment, lithography process, and silane surface treatment. Fig. 1(a) illustrates the fabrication flow chart of the multilayered polymeric RF biosensor. The PEN polymer substrate was initially cleaned by acetone solution with ultrasonic agitation for 10 min, and rinsed in isopropyl alcohol (IPA) solution for 3 min. The surface of the biochip was subsequently dried out using an N_2 spray gun, as illustrated in Fig. 1(a)-(I). The dimension of the prepared PEN polymeric substrate was approximately 5 cm^2. The surface of the polymeric substrate was treated with O_2 plasma by RIE (SAMCO RIE 10N) before the metal deposition process. Titanium and copper were used as the seed layer and the structure material, which deposited a thickness of 500 and 5000 Å on the PEN flexible substrate by an E-beam evaporator (ULVAC EGK-3M). The surface roughness of the deposited metal layer was approximately 12 Å by a surface profile measuring machine (TENCO, AS500 Alpha-Step). The geometry of the designed biosensor on the metal structures layer was defined by the lithography and wet etching processes, as illustrated in Fig. 1(a)-(II) and (III). Consequently, Parylene-C, which may be a dielectric material or passivation layer of the proposed biosensor, was deposited on the surface of the etched Ti/Cu metal layer by a Parylene deposition system (La-Chi LH300). The thickness of the Parylene layer was approximately 3 μm, and the surface roughness of the Parylene layer was approximately 3.5 nm, as illustrated in Fig. 1(a)-(IV). The Silane A-174 (La-Chi Enterprise Co., Ltd., Taiwan) was used in this study to enhance the adhesion force between the Parylene-C thin film and the PEN flexible substrate. The silane A-174 diluted solution was composed of IPA solution, DI water, and silane A-174 solution. The volumetric percentages of the IPA solution, DI water, and pure silane A-174 solution were 100 ml, 100 ml, and 1 ml, respectively. The fabricated biosensor was subsequently immersed in the diluted solution for 20 min, rinsed with IPA solution for 3 min, and dried under N_2. The fabrication procedures, which include O_2 plasma treatment, metal deposition, and lithography, may be repeated for deposition of the second polymer and metal layer, as illustrated in Fig. 1(a)-(V). The thickness of the second Ti/Cu metal layer was approximately 2000 and 20,000 Å. The upper metal layer must deposit over 2 μm of total thickness to avoid the skin depth effect. The electric current mainly flows at the skin of the conductor, at an average depth that is referred to as the skin depth. The thickness of the transmission metal layer must be higher than the skin depth to avoid the signal loss (Kuanr et al., 2003). Fig. 1(a)-(VI) illustrates the final process of the proposed polymeric biosensor. The geometry of the sensing CPW structures for DNA detection can further be defined after etching the upper metal of the biochip. However, for DNA hybridization and immobilization procedures, a layer of gold metal with a thickness of 2000 Å covered the surface of the upper etched copper layer. The three-dimensional illustration of the multilayered polymeric RF biosensor is displayed in Fig. 1(b). Fig. 1(c) displays an overview SEM photograph of the polymeric biosensor that was captured by an FE-SEM (HITACHI, S4300) in ITRC, Taiwan.

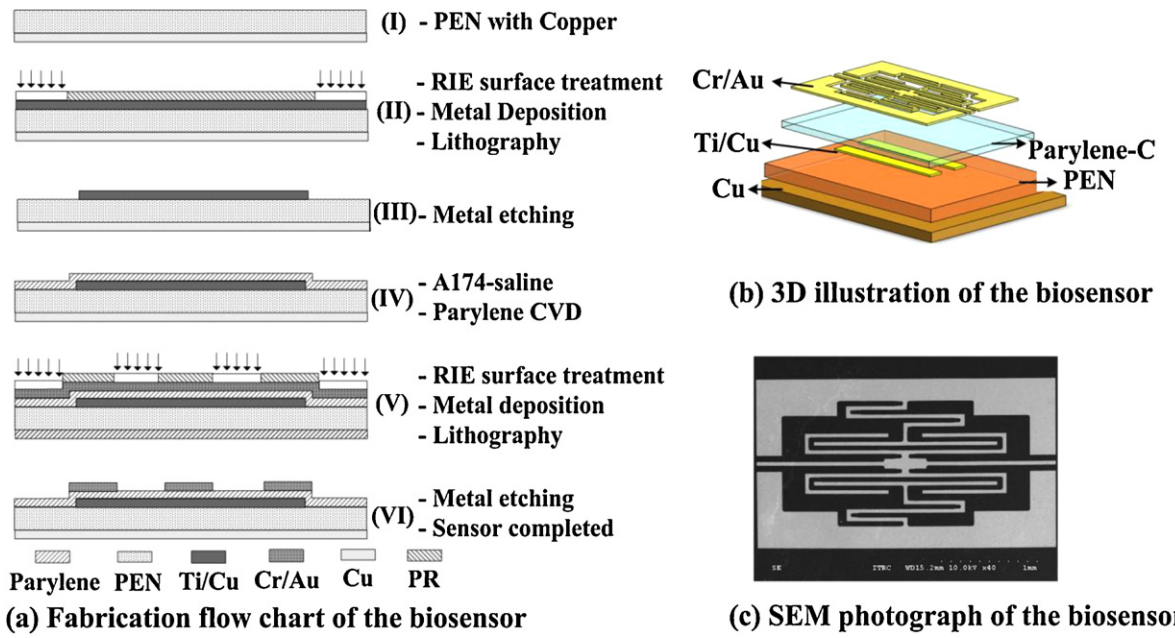

Fig. 1. Photographs of the developed polymeric biosensor. (a) Fabrication flow chart of the polymeric biosensor; (b) 3D illustration of the biosensor; (c) SEM photograph of the biosensor.

2.2. Surface modification for Parylene-C

This study used surface modification for immobilizing the conjugate AuNPs–DNA molecular on the proposed polymeric surface of the biochip. Thioglycolic acid (TGA) is the organic compound that contains both a thiol and a carboxylic acid. The purpose of using the TGA reagent was to modify and form the thiol-group on the surface of Parylene-C. Fig. 2(a) exhibits the mechanism of the TGA chemical reaction for surface modification. Hydrochloric acid was the product of the chemical reaction in the TGA surface modification. Therefore, the modified biochip must be washed by DI water and DD water repeatedly until the pH value of DI water reaches the range of 6.8–7.2. The pH value of the washed DI water was changed to approximately 6 by washing three times. The modified biosensor was subsequently washed twice by DD water to change the pH value to approximately 7. The original chlorine group of the Parylene-C surface may be replaced by the thiol group in the TGA surface modification process. According to the experimental results, the optimal concentration ratio of the chemical reagent between Parylene and TGA was one to three. The favorable experimental condition was approximately 60 °C for 12 h.

To evaluate the effect of surface modification by the TGA reagent, the modified polymeric biochip was immersed in the solutions that contained gold nanoparticles (13 nm diameter) or magnetic nanoparticles (8 nm diameter) for 24 h, and subsequently rinsed with DI water and dried under N_2. Fig. 2(b) displays the SEM photographs of the modified surface of the biochip that immobilized gold and magnetic nanoparticles, respectively. The distribution of the immobilized nanoparticles on the modified polymeric surface of the biochip is observed, and the successful surface modification by the TGA chemical reagent to form a thiol group on the surface of the biochip is demonstrated, which may immobilize the gold or modified magnetic nanoparticles for subsequent DNA detection.

2.3. DNA hybridization with self-assembly multilayer AuNPs

The gold nanoparticles were immobilized on the surface of the polymeric biosensor for radio frequency detection, and a multilayer AuNPs structure was used over the sensing areas to obtain a measurable frequency shift of the biosensor after oligonucleotide hybridization. The sequences of the probe DNA (pDNA), target DNA (tDNA), and capture DNA (cDNA) are illustrated in Table 1. All of the single strand DNA (ssDNA) biomolecules and functional nanoparticles, including AuNPs and MNPs, were obtained from TANbead Biological Corp. and MDbio Inc. (Taiwan). We first prepared the solutions of the single-strand thiol-modified pDNA and cDNA that were immobilized on the surface of AuNPs for the immobilization and hybridization procedures. In the solutions, the thiol group has a particular affinity for gold by a binding van der Waals force. Therefore, the thiol-modified pDNA and cDNA may be immobilized on the surface of AuNPs by the binding van der Waals force.

The procedures of the DNA hybridization with multilayered gold nanoparticles are illustrated in Fig. 2(c). The diameter of the AuNPs was approximately 13 ± 2 nm. The surface of the polymeric biosensor must first be modified by a TGA thiol-modified solution to form a thiol group on the Parylene surface. Subsequently, the biochip may be immersed into a conjugate cDNA–AuNPs solution for 24 h to establish monolayer AuNPs on the thiol-modified surface of the biochip, and rinsed with a PBS solution for 3 min. The phosphate-buffered saline (PBS) solution was used as a washing buffer in this study. The PBS solution contained a NaCl and NaH_2PO_4 solution with a pH value of 7.4.

The polymer-based biochip was dripped with 10 μl of target ssDNA solution for 30 min after the establishment of the monolayer AuNPs with cDNA. The stored solution of the target DNA fragments was diluted in the washing buffer to 0.1 μM. The concentration of the target solution was further diluted according to the experimental requirement of 10 nM, 1 nM, 100 pM, 10 pM, and 1 pM. The sensing biochip was subsequently dripped with 20 μl of pDNA–AuNPs solution that contained the thiol-modified probe DNA that was immobilized on the surface of AuNPs, and rinsed by a PBS solution for 3 min. The second-layer of the AuNPs structure

Table 1
The sequences of the capture, probe, and target DNA.

Name	Sequence
Capture DNA	3′-HS-AAAAAAAAAACCTAATAACAAT-5′
Probe DNA	3′-TTATAACTATTCCTAAAAAAAAAAA-SH-5′
Target DNA	5′-GGATTATTGTTAAATATTGATAAGGAT-3′

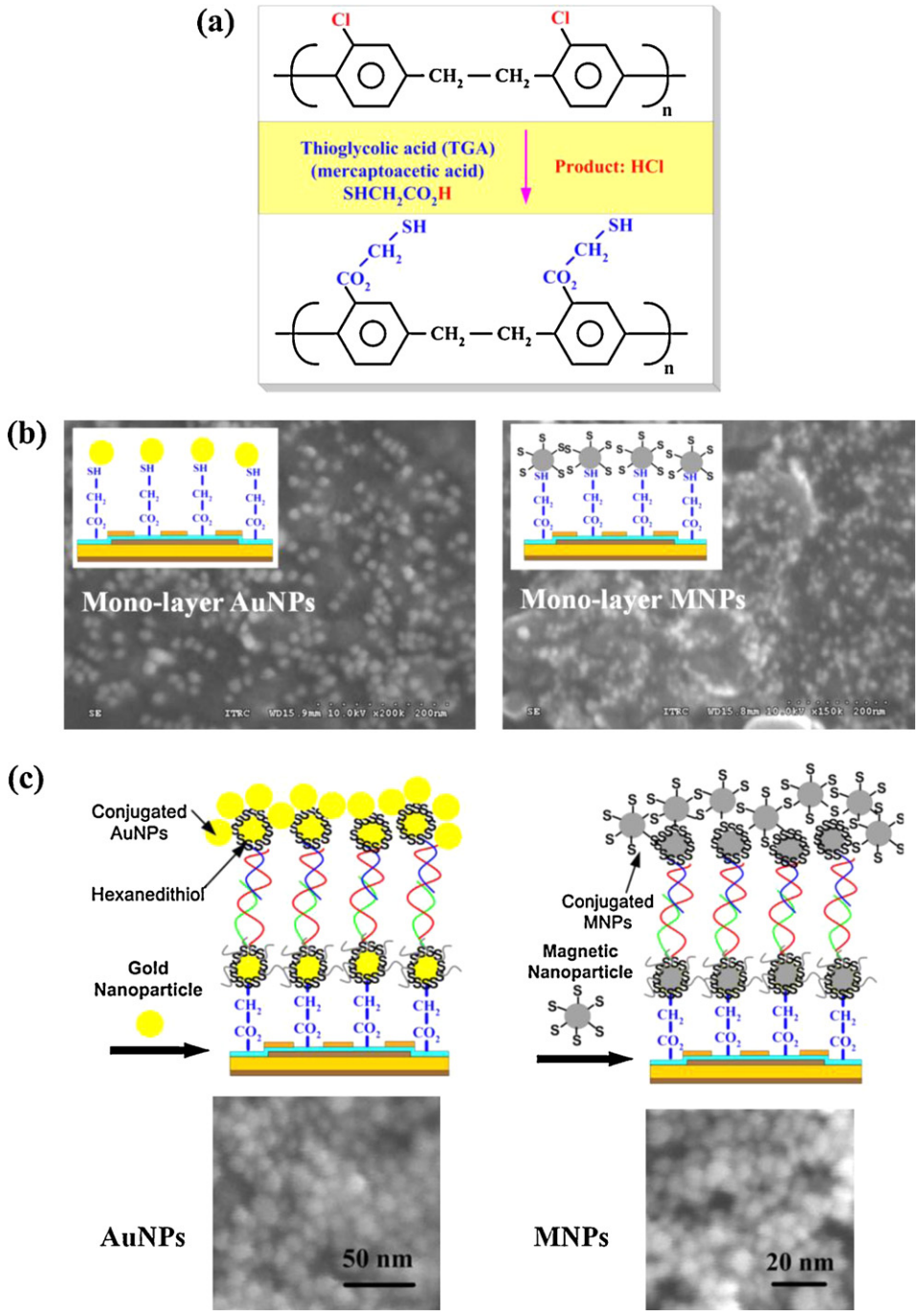

Fig. 2. Illustration of surface modification and SEM photographs of functional nanoparticles immobilization and hybridization on the modified biochips: (a) mechanisms of surface modification with TGA (Experimental parameter – Parylene: TGA = 1:3 at 60 °C for 12 h); (b) immobilization of the mono-layer AuNPs and MNPs on the modified biochip; (c) illustrations of the triple-layer AuNPs and MNPs by hybridization procedures.

was subsequently established by manual pipetting for 30 min, and the no hybridized target DNA, probe DNA, and second-layer AuNPs were rinsed by using the washing solution.

Subsequently, a hexandithiol solution was used to modify the surface of the second-layer AuNPs. The chemical compound hexandithiol contains thiol at both ends of the molecule. One end attaches to the second-layer of the AuNPs surface, and the other end may be used to establish a third layer of AuNPs. Consequently, the biochip may be immersed in an AuNPs solution for 24 h to form triple-layer self-assembly AuNPs, and subsequently rinsed by PBS solution for 3 min and dried by N_2 gas to remove the suspending AuNPs, as demonstrated in Fig. 2(c). The gold nanoparticles were not continuously distributed on the biosensor. However, the distribution of the triple-layer gold nanoparticles was markedly denser than that of the double-layer.

2.4. DNA hybridization with self-assembly multilayer MNPs

The procedures of DNA hybridization with multilayer magnetic nanoparticles are illustrated in Fig. 2(c). The diameter of the MNPs was approximately 8 ± 1 nm. The experimental procedures are detailed in this section. The sequence of the cDNA, tDNA, and

pDNA are mentioned in the last section of this paper. In general, the MNPs are considered a vital class of materials in the fields of nanotechnology and biotechnology because of their potential opportunities for DNA and protein detection applications. Therefore, the MNPs were used for DNA detection in this study to investigate the feasibility of the RF DNA detection method by using self-assembly multilayer MNPs on the polymeric biosensor.

The same procedure for establishing a multilayer AuNPs structure was used to establish multilayer MNPs. The distribution of the triple-layer magnetic nanoparticles was markedly denser than that of the double-layer magnetic nanoparticles, as illustrated in the SEM photographs of Fig. 2(c).

3. Results and discussion

3.1. Measurement and simulation results

This section presents the comparison of the experimental results on the polymer biosensors with the simulations. The scattering parameter of the fabricated biochip was measured to verify the design of the developed biochip. The scattering parameters from the simulated results were obtained by using a method of momentum in the simulation tool of the advanced design system (ADS). The measured result was observed on an RF measurement system that included a network analyzer and a probe station to measure the characteristics of the developed biosensor. The model number of the network analyzer (NA) is Agilent E5071C. The measuring frequency limit of the NA is in the range of 100 KHz–8 GHz. Therefore, the measuring frequency range of the developed biochip was 100 KHz–8 GHz. The probe station was applied to the aligner and probe on the electrodes of the biochip by using a CCD camera and Ground-Signals-Ground (G-S-G) microprobes. The gap distance between the ground and the signal probes of the microprobes was 100 μm. This distance must be considered in the design of the biosensor because the gap distance of the electrodes of the biosensor must be consistent to that of the GSG microprobes. The radio frequency signals may be transmitted between the NA and the biosensor through the coaxial cable signal and GSG microprobe. Furthermore, the measuring results of the scattering parameter were displayed on the NA screen, and the required results were marked and exported for further analysis.

Fig. 3(a) illustrates the measured and simulated signal response of the proposed biosensor. The difference of the signal response between the measured and simulated results was dependent on the fabrication batches, and a slight variation of the central frequency between 6.3 and 6.5 GHz was observed. The electromagnetic characteristic of this polymer biosensor was a band-stop filter, and the center frequency was approximately 6.4 GHz.

This simulation of the biosensor was conducted without considering nanoparticles, chemical reagents, and molecules. The comparison of the simulated results and measuring results indicate that their center frequencies may be distinguishable. The center frequencies of the simulated and measuring results were consistent and the trend of the measuring results was similar to that of the simulation results. However, the change of the center frequency between the measuring and simulated results was approximately 0.2 GHz. The change of the center frequency was related to the change of the geometry of biosensor from the fabrication process. It slightly altered the geometries of the fabricated biosensor. Consequently, the center frequency of the proposed biosensor changed in conjunction with the coupling capacitance and inductance of the fabricated biochip.

3.2. DNA detection using AuNPs and MNPs

The gold nanoparticles of DNA detection may be formed as multilayered AuNPs structures, which can enhance the performance of the polymer biosensor in the detection procedures. The gold nanoparticles of the double-layer and triple-layer are immobilized on the biosensor by the tNDA hybridization procedures. The shift of the center frequency increases in conjunction with the number of the used AuNPs. However, the number of the AuNPs that were immobilized on the surface of the biochip was dependent on the concentration of the tDNA solution. Therefore, the comparison among the various concentrations of tDNA was vital to the results for DNA detection in this study. The selected tDNA concentrations were 10 nM, 1 nM, 100 pM, 10 pM, and 1 pM. The S-parameters of the developed biosensors with the conjugate DNA–AuNPs were measured by a radio frequency measurement system. The shift of the center frequency was vital in this study, and was a valuable index for determining the existence of the AuNPs–DNA or the MNPs–DNA in the biosensor. Conversely, the shift of the center frequency was an appropriate index of the RF biosensor because the existence of the bio-molecules with functional nanoparticles may alter the center frequency of the RF biosensor. The sensitivity may be represented in the amplitude of the shifted center frequency. The measured results of the AuNPs that enhanced the DNA detection in the tDNA concentrations of 100 pM are illustrated in Fig. 3(b). The shift of the center frequency increased in conjunction with the number of NPs layers at the same tDNA concentrations. The shifts of the center frequency of the triple, double, and single AuNPs were 0.26 GHz, 0.2 GHz, and 0.3 GHz, respectively. The shift of the center frequency was more sensitive to the triple AuNPs layer than the double AuNPs layer. The single AuNPs layer immobilized the AuNPs only on the surface of the biosensor without any biomolecules. Therefore, conjugated triple AuNPs–DNA obtained a superior sensitive frequency shift. The triple NPs layer structure may be used to enhance the sensitivity of the biosensor to determine the detection limit of the proposed biosensor. The shift of the center frequency may be observed at a low concentration of the tDNA.

This study used gold nanoparticles and MNPs to enhance the biodetected performance. The shift of the center frequency increased in conjunction with the number of MNPs, which also changes the insertion loss. This phenomenon of changed insertion loss depends on the electromagnetic absorption characteristic of the magnetic nanoparticles. In addition, the shift of the center frequency may be changed because the permeability and permittivity change by using MNPs. Therefore, the inductance and capacitance of the biosensor may be altered by immobilizing MNPs on the surface of the biosensor. The concentration of the target DNA affected the number of the immobilized MNPs on the surface of the biosensor. Hence, the comparison among the various concentrations of the tDNA is vital for DNA detection. The concentrations of the tDNA solution for DNA detection in this study were 10 nM, 1 nM, 100 pM, 10 pM, and 1 pM. The measured results of the DNA detection that was enhanced by the MNPs in the concentrations of 100 pM tDNA solution are illustrated in Fig. 3(c). The shift of the center frequency indicated that the triple MNPs layer was more sensitive than the double MNPs layer. The shifts of the center frequency of the triple, double, and single AuNPs were 0.26 GHz, 0.2 GHz, and 0.3 GHz, respectively. The decrease in the S parameter S21 was dependent on the sensor layer numbers for the MNPs, but not for the AuNPs. The MNPs exhibited electromagnetic absorption characteristics, and the insertion loss of the S parameter decreased with the number of the MNPs layer (Lee and Chen, 2007).

The measured results were expressed as FG_1, FG_2, and FG_3 to compare the shifted frequency of the biosensor with triple-layer, double-layer, and monolayer AuNPs. The FG_1, FG_2, and FG_3 denote the values of the measured shifted center frequency

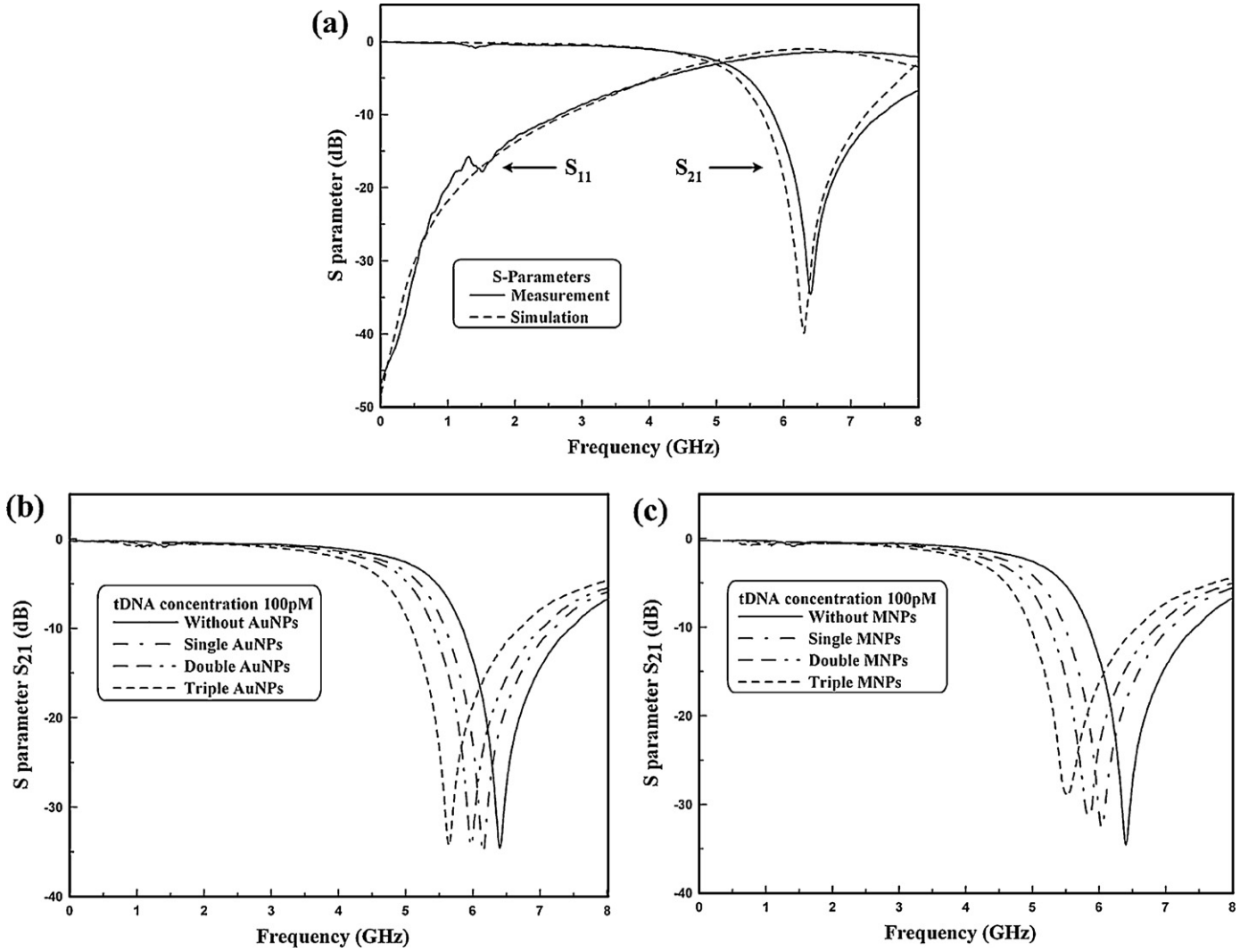

Fig. 3. Scattering parameter measurement and simulation results: (a) simulation and measurement results of the developed RF biosensor; (b) the S_{21} frequency response of the DNA detection using triple-layer, double-layer, and single layer AuNPs at tDNA concentration of 100 pM; (c) the S_{21} frequency response of the DNA detection using triple-layer, double-layer, and single layer MNPs at tDNA concentration of 100 pM.

after the mono-layer, double-layer, and triple-layer of AuNPs with DNA were established, respectively, and $FG_{w/o}$ denotes the measured shifted frequency of the biosensor without the immobilized AuNP–DNA structure. We also used FM_1, FM_2, and FM_3 to express the measured results for DNA detection with MNPs. The FM_1, FM_2, and FM_3 denote the values of the measured shifted center frequency after the establishment of mono-layer, double-layer, and triple-layer of MNPs, respectively. The $FM_{w/o}$ denotes the measured frequency shift of the biosensor without the immobilized MNPs–DNA structure. The detection results of the various tDNA concentrations of 10 nM, 1 nM, 100 pM, 10 pM, and 1 pM generalize the shifted center frequencies of the polymer biosensor with AuNPs and MNPs, as illustrated in Fig. 4(a and b). The results indicated that the center frequency shift was more sensitive to the number of NPs layers than to the concentration of the target DNA. The curve of the FG_3 and FM_3 reduces faster than FG2 and FM2, and even faster than FG1 and FM1, as the target DNA concentration increases.

The shifted center frequency of multilayer AuNPs and MNPs is greater than that of monolayer AuNPs. The multilayer nanoparticles that were composed of a higher tDNA concentration of 10 nM exhibited a larger shifted center frequency than those with a lower tDNA concentration. Although the triple-layer AuNPs that used a tDNA concentration of 1 pM may be detected in the DNA detection with both AuNPs and MNPs, they cannot be clearly distinguished. However, the sensitivity of double-layer AuNPs and MNPs with 10 pM of DNA solution may be distinguished from the double-layer and triple-layer enhancement.

ΔFG_{21}, ΔFG_{32}, ΔFM_{21}, and ΔFM_{32} were used to present the differences of the shifted frequency by using triple-layer, double-layer, and monolayer MNPs–DNA and AuNPs–DNA conjugate structures. The definitions of ΔFG_{21}, ΔFG_{32}, ΔFM_{21}, and ΔFM_{32} are described by the following equations:

$$\Delta FG_{21} = FG_2 - FG_1 \quad (1)$$

$$\Delta FG_{32} = FG_3 - FG_2 \quad (2)$$

$$\Delta FM_{21} = FM_2 - FM_1 \quad (3)$$

$$\Delta FM_{32} = FM_3 - FM_2 \quad (4)$$

If the shifted frequency of the mono-layer and double-layer MNPs and AuNPs on the biosensor are used as the references, the shifted frequencies of the various tDNA concentrations may be further diagramed by using the parameters of ΔFG_{21}, ΔFG_{32}, ΔFM_{21}, and ΔFM_{32}, as illustrated in Fig. 5. The shifted center frequency of the triple-layer AuNPs is greater than that of double-layer AuNPs.

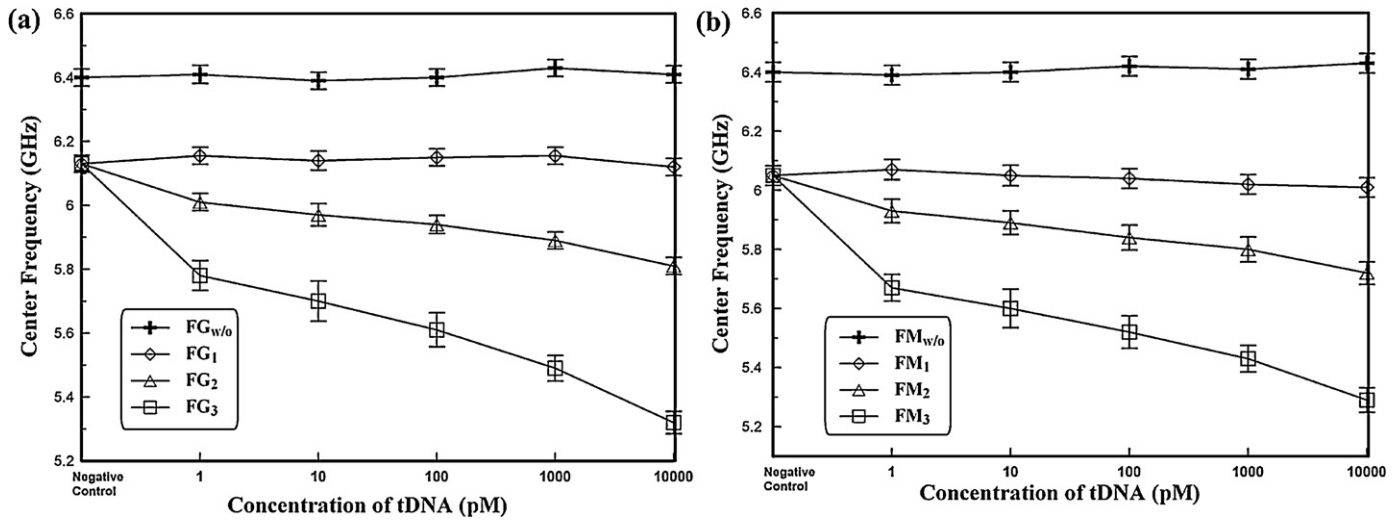

Fig. 4. Measurements of the center frequency shift using AuNPs and MNPs with various tDNA concentrations: (a) the center frequency of self-assembly AuNPs versus various tDNA concentrations; (b) the center frequency of using self-assembly MNPs versus various tDNA concentrations. (The FG_1, FG_2 and FG_3 denote the S_{21} response of mono-layer, double-layer and triple-layer AuNPs structures, respectively; the FM_1, FM_2, and FM_3 denote S_{21} response of mono-layer, double-layer and triple-layer MNPs structures, respectively.)

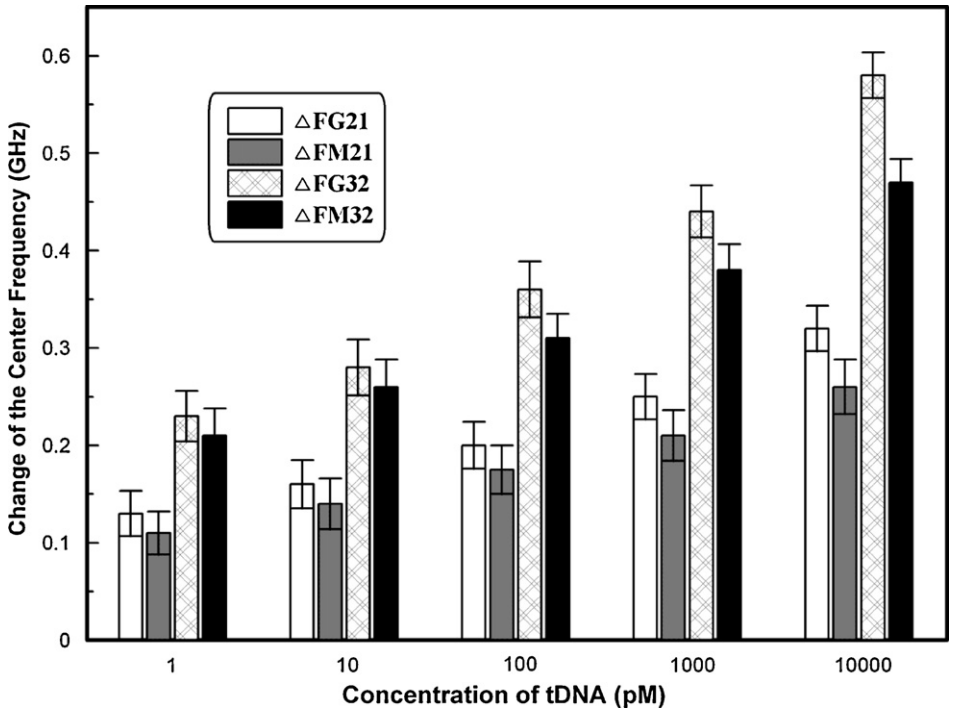

Fig. 5. Comparison of the shifted frequency measurement of multilayer AuNPs and MNPs for DNA detection. (ΔFG_{21}, ΔFG_{32}, ΔFM_{21}, and ΔFM_{32} are used to present the differences of the shifted frequency using triple-layer, double-layer, and monolayer MNPs–DNA and AuNPs–DNA conjugate structures. FG denotes center frequency shifts by using AuNPs. FM denotes center frequency shifts by using MNPs.)

The shifted frequency may be increased further by using a higher tDNA concentration. The error bars in Figs. 4 and 5 illustrate the 95% confidence intervals. In comparison to the previous RF biosensor studies (Chien et al., 2008; Kim et al., 2006), this study is the first to present DNA detection with MNPs by using a radio frequency method. As illustrated in Fig. 5, the ΔFG_{32} is progressively greater than the ΔFM_{32} as the tDNA concentration increases, which indicates that the AuNPs are more appropriate than MNPs for use in the developed RF DNA detection system. Conversely, the AuNPs are superior, even though the MNPs may be used in the RF DNA detection system. In Fig. 5, the sensing error bars range of the ΔFG_{32} and ΔFM_{32} are approximately 0.1 GHz, and the shifted frequency of the ΔFG_{32} and ΔFM_{32} may be displayed over 0.1 GHz at the 100 fM–1 pM tDNA concentration. Therefore, the lower detection limit of the developed RF biosensor is approximately 500 fM. The experimental upper detection limit of the biosensor is approximately 10 nM. According to the measured results, the feasibility of DNA detection enhanced by AuNPs and MNPs on the developed polymeric RF biosensor was completed successfully.

4. Conclusion

In summary, a multilayered polymeric DNA biochip using radio frequency detection was developed in this study. This developed

biosensor used two polymer layers and two copper transmission layers as multilayered RF DNA biochip that may provide advantages of the small chip-size and highly sensitivity. The two copper transmission structures can increase the sensing area that was added from the single capacitor structure to the double capacitor structures, and the sensitivity may be further enhanced. Moreover, the study used gold nanoparticles and magnetic nanoparticles to enhance the sensitivity of the biosensor. The multilayered nanoparticles on the biosensor affect the electromagnetic characteristics of the RF biosensor. Therefore, the center frequency of the biosensor was shifted by using gold nanoparticles and magnetic nanoparticles.

The following conclusions are based on the experimental results. First, a multilayered polymeric DNA biochip using MEMS, RF, and biochemical methodology was successfully developed. Second, the miniaturization of the RF biosensor may be effectively achieved through the multilayered CPW structure. Subsequently, the price of a single biochip may be substantially lowered by using polymeric material, which offers the possibility to replace common glass and silicon wafers. Finally, the shifts of the center frequency by using AuNPs and MNPs triple-layer were approximately 0.9 and 0.7 GHz, which exceeded the shift of the double-layer AuNPs and MNPs by 0.6 and 0.5 GHz, respectively. In a comparison of the previous RF DNA detection with similar tDNA, the shifts of center frequency were larger than those of the previous RF DNA biosensor (Chien et al., 2008). The developed RF biosensor was more sensitive for DNA detection at the same response frequency than that of the previous study.

The multilayered polymeric RF DNA biosensor with the AuNPs and MNPs provides a powerful and evolving toolkit for designing an ultrasensitive detection method. Compared to the conventional biosensor, the developed polymeric biosensor may offer an inexpensive, disposable, and highly sensitive option for biomedicine diagnostic systems (Hong et al., 2010; Chien et al., 2008; Kim et al., 2008; Sharifi et al., 2009). The developed biosensor offers notable potential as a field-based device for the diagnosis of diseases and for healthcare applications because of the current widespread use of biomedical detection systems.

Acknowledgments

The authors wish to thank the National Taiwan University NEMS Center and National Normal Taiwan University MOEMS Laboratory for providing experimental facilities. We deeply appreciate the financial support offered by the National Science Council (NSC) of Taiwan, Republic of China, under contract NSC 99-2221-E-002-081-MY3.

References

Agasti, S.S., Rana, S., Park, M.H., Kim, C.K., You, C.C., Rotello, V.M., 2010. Adv. Drug Deliv. Rev. 62, 316–328.
Alivisatos, P., 2004. Nat. Biotechnol. 22, 47–52.
Anderson, D.G., Putnam, D., Lavik, E.B., Mahmood, T.A., Langer, R., 2005. Biomaterials 26, 4892–4897.
Blacklock, J., You, Y.Z., Zhou, Q.H., Mao, G., Oupicky, D., 2009. Biomaterials 30, 939–950.
Chang, T.Y., Yadav, V.G., Leo, S.D., Mohedas, A., Rajalingam, B., Chen, C.L., Selvarasah, S., Dokmeci, M.R., Khademhosseini, A., 2007a. Am. Chem. Soc. 10, 1021–1030.
Chang, T.L., Tsai, C.Y., Sun, C.C., Chen, C.C., Kuo, L.S., Chen, P.H., 2007b. Biosen. Bioelectron. 22, 3139–3145.
Chien, J.H, Chen, P.H., Kuo, L.S., 2007. Appl. Phys. Lett. 91, 143901.
Chien, J.H., Yang, C.H., Chen, P.H., Yang, C.R., Lin, C.S., Wang, H., 2008. Front. Biosci. 13, 4756–4764.
Drummond, T.G., Hill, M.G., Barton, J.K., 2003. Nat. Biotechnol. 21, 1192–1199.
Giljohann, D.A., Mirkin, C.A., 2009. Nature 462, 461–464.
Giljohann, D.A., Seferos, D.S., Daniel, W.L., Massich, M.D., Patel, P.C., Mirkin, C.A., 2010. Angew. Chem. Int. Ed. 49, 3280–3294.
Huang, G.S., Lin, Y.S., Wang, C.H., Chen, C.H., 2009. IEEE Trans. Microw. Theory Tech. 57, 807–814.
Hong, C.C., Chang, P.H., Lin, C.C., Hong, C.L., 2010. Biosens. Bioelectron. 25, 2058–2064.
Kim, Y.I., Park, T.S., Kang, J.H., Lee, M.C., Kim, J.T., Park, J.H., Baik, H.K., 2006. Sens. Actuators B 119, 592–599.
Kim, Y.S., Kim, J.H., Kim, I.A., Lee, S.J., Gu, M.B., 2011. Biosens. Bioelectron. 26, 4058–4063.
Kim, Y.H., Yoon, S.I., Park, S.C., Lim, D.H., Jung, H.I., Kim, Y.J., 2008. Sens. Actuators B 130, 823–828.
Lee, C.C., Chen, D.W., 2007. Appl. Phys. Lett. 90, 193102.
Kuanr, B., Malkinski, L., Camley, R.E., Celinski, Z., 2003. J. Appl. Phys. 93, 8591–8593.
Mallard, F., Marchand, G., Ginot, F., Campagnolo, R., 2005. Biosens. Bioelectron. 20, 1813–1820.
Nam, J.M., Stoeva, S.I., Mirkin, C.A., 2004. J. Am. Chem. Soc. 126, 5932–5933.
Pal, S., Alocilja, E.C., 2010. Biosens. Bioelectron. 26, 1624–1630.
Park, S.J., Taton, T.A., Mirkin, C.A., 2002. Science 295, 1503–1506.
Perng, J.K., Hunt, W.D., Edmonson, P.J., 2007. IEEE Sensor Conf., 691–694.
Ratner, B.D., Bryant, S.J., 2004. Annu. Rev. Biomed. Eng. 6, 41–75.
Sharifi, H., Lahiji, R.L., Lin, H.C., Ye, P.D., Katehi, P.B., Mohammadi, S., 2009. IEEE Trans. Adv. Packag. 32, 84–92.
Sheehan, P.E., Whitman, L.J., 2005. Nano Lett. 5, 803–807.
Stoeva, S.I., Lee, J.S., Thaxton, C.S., Mirkin, C.A., 2006. Angew. Chem.-Int. Edit. 45, 3303–3306.
Schotter, J., Kamp, P.B., Becker, A., Puhler, A., Reiss, G., Bruckl, H., 2004. Biosens. Bioelectron. 19, 1149–1156.
Tirrel, M., Kokkoli, E., Biesalski, M., 2002. Surf. Sci. 500, 61–83.
Tokonami, S., Shiigi, H., Nagaoka, T., 2008. Anal. Chem. 80, 8071–8075.
Tsai, C.Y., Chang, T.L., Kuo, L.S., Chen, P.H., 2006. Appl. Phys. Lett. 89, 203902.
Wang, L., Liu, Q., Hu, Z., Zhang, Y., Wu, C., 2009a. Talanta 78, 647–652.
Wang, Y., Chen, M., Zhang, L., Ding, Y., Luo, Y., Xu, Q., Shi, J., Cao, L., Fu, W., 2009b. Biosens. Bioelectron. 24, 3455–3460.
Zheng, J., Webster, J.R., Mastrangelo, C.H., Ugaz, V.M., Burns, M.A., Burke, D.T., 2007. Sens. Actuators B 125, 343–351.